



Since January 2020 Elsevier has created a COVID-19 resource centre with free information in English and Mandarin on the novel coronavirus COVID-19. The COVID-19 resource centre is hosted on Elsevier Connect, the company's public news and information website.

Elsevier hereby grants permission to make all its COVID-19-related research that is available on the COVID-19 resource centre - including this research content - immediately available in PubMed Central and other publicly funded repositories, such as the WHO COVID database with rights for unrestricted research re-use and analyses in any form or by any means with acknowledgement of the original source. These permissions are granted for free by Elsevier for as long as the COVID-19 resource centre remains active.



The non-pharmaceutical interventions may affect the advantage in transmission of mutated variants during epidemics: A conceptual model for COVID-19



Shi Zhao^{a,b,*}, Kai Wang^c, Marc K.C. Chong^{a,b}, Salihu S. Musa^{d,e}, Mu He^f, Lefei Han^{g,*}, Daihai He^{d,*,1}, Maggie H. Wang^{a,b,1}

^aJC School of Public Health and Primary Care, Chinese University of Hong Kong, Hong Kong, China

^bCUHK Shenzhen Research Institute, Shenzhen, China

^cDepartment of Medical Engineering and Technology, Xinjiang Medical University, Urumqi, China

^dDepartment of Applied Mathematics, Hong Kong Polytechnic University, Hong Kong, China

^eDepartment of Mathematics, Kano University of Science and Technology, Wudil, Nigeria

^fDepartment of Foundational Mathematics, Xi'an Jiaotong-Liverpool University, Suzhou, China

^gSchool of Global Health, Chinese Center for Tropical Diseases Research, Shanghai Jiao Tong University School of Medicine, Shanghai, China

ARTICLE INFO

Article history:

Received 1 September 2021

Revised 15 March 2022

Accepted 18 March 2022

Available online 21 March 2022

Keywords:

COVID-19

Transmission advantage

Non-pharmaceutical intervention

Reproduction number

Mathematical modelling

ABSTRACT

As the COVID-19 pandemic continues, genetic mutations in SARS-CoV-2 emerge, and some of them are found more contagious than the previously identified strains, acting as the major mechanism for many large-scale epidemics. The transmission advantage of mutated variants is widely believed as an innate biological feature that is difficult to be altered by artificial factors. In this study, we explore how non-pharmaceutical interventions (NPI) may affect transmission advantage. A two-strain compartmental epidemic model is proposed and simulated to investigate the biological mechanism of the relationships among different NPIs, the changes in transmissibility of each strain and transmission advantage. Although the NPIs are effective in flattening the epidemic curve, we demonstrate that NPIs probably lead to a decline in transmission advantage, which is likely to occur if the NPIs become intensive. Our findings uncover the mechanistic relationship between NPIs and transmission advantage dynamically, and highlight the important role of NPIs not only in controlling the intensity of epidemics but also in slowing or even containing the growth of the proportion of variants.

© 2022 Elsevier Ltd. All rights reserved.

1. Introduction

The coronavirus disease 2019 (COVID-19), caused by the severe acute respiratory syndrome coronavirus 2 (SARS-CoV-2) (Hu et al., 2021), poses a serious threat to global health (Li et al., 2020; Wu et al., 2020). The control of COVID-19 requires the knowledge of the factors that affect the transmission process (Kutter et al., 2018; Fraser et al., 2004), e.g., virus mutation is one of the major challenges (Baum et al., 2020; Tsetsarkin et al., 2007). For instance,

around September 2020, genetic variants in B.1.1.7 lineage were firstly detected in the United Kingdom (UK) (Tang et al., 2020), then spread to elsewhere globally, and trended to reach fixation rapidly in many places, e.g., South Africa (Tang et al., 2021), Brazil (Claro et al., 2021), the US (Galloway et al., 2021), and the UK (Leung et al., 2021). In Brazil, the variants in P.1 lineage, or the variant of concern 202101/02 (England, 2021), become prevalent in many places including the UK and Brazil (Wise, 2021). In India, the recent B.1.617 lineage emerged and resulted in large numbers of case and deaths locally, which is considered as a potential risk for many other places globally. These emerging variants may affect the epidemiological characteristics of COVID-19 (Walensky et al., 2021; Rondinone et al., 2021), and the protective effects of vaccines in use or under development (Xie et al., 2021; Moore and Offit, 2021; Muik et al., 2021; Supasa et al., 2021; Yadav et al., 2021).

For a mutated variant that may be more infectious, one of the key investigations to find how much more transmissible are these variants than another type of variants, typically the predecessor (original) variants. The increase in the transmissibility

* Corresponding authors at: JC School of Public Health and Primary Care, Chinese University of Hong Kong, Hong Kong, China (S. Zhao); School of Global Health, Chinese Center for Tropical Diseases Research, Shanghai Jiao Tong University School of Medicine, Shanghai, China (L. Han); Department of Applied Mathematics, Hong Kong Polytechnic University, Hong Kong, China (D. He).

E-mail addresses: zhaoshi.cmsa@gmail.com (S. Zhao), marc@cuhk.edu.hk (M.K.C. Chong), salihu-sabiu.musa@connect.polyu.hk (S.S. Musa), mu.he@xjtu.edu.cn (M. He), lifan@sjtu.edu.cn (L. Han), daihai.he@polyu.edu.hk (D. He), maggiew@cuhk.edu.hk (M.H. Wang).

¹ DH, and MHW are joint senior authors.

attributed to the mutated variants is named transmission advantage, which is a relative quantity measuring the fitness of pathogen at a population scale. Epidemiological studies reported transmission advantage in many of the mutated SARS-CoV-2 variants (Davies et al., 2021; Volz et al., 2021a; Zhao et al., 2021a,b; Leung et al., 2021), which is considered as the major reason for the large-scale outbreaks in many places despite the controlling efforts implemented previously. Regardless of the widely implemented non-pharmaceutical interventions (NPI), which are adopted to mitigate epidemics, the mutated variants continuously bring challenges to COVID-19 control. It is widely believed (and adopted) that the transmission advantage of a mutated variant is a biological feature, which holds constantly and cannot be altered by artificial factors. However, interestingly, a recent ecological study reported that the transmission advantage of B.1.1.7 variants declined in England around December 2020 empirically (Graham et al., 2021), which coincides with numbers of intensive control measures implemented simultaneously, e.g., social distancing and regional lockdown. Inspired by this coincidence, we suspect that NPIs play a role in affecting the transmission advantage.

To explore how NPIs may determine transmission advantage, we formulate a classic two-strain compartmental model to investigate the biological mechanism of the relationship between different NPIs and the change in transmissibility of each strain. We simulate this model to demonstrate that several types of NPIs could affect the effective transmission advantage dynamically under various scenarios accounting for the impacts of each NPI.

2. Model

2.1. Model formulation

2.1.1. Conceptualization and parameterization

We develop a compartmental model based on the classic susceptible-exposed-infectious-removed ('SEIR') modelling structure. The susceptible population is denoted by S . The infections are divided into 2 stages including exposed (E) and infectious (A and I) cases. Specifically, the infections in class E are corresponding to the cases during latent period (σ^{-1}). After the latent period, we consider 2 classes of infectious cases including asymptomatic or with sub-clinical conditions (A), and symptomatic (I) cases, both of whom are infectious. The removed (by recovery or death) population is denoted by R .

The transmission is driven by the contact between susceptible (S) and infectious (A and I) individuals at an effective contact rate (or transmission rate) β . All infected individuals join class E immediately after infection, and then become infectious by leaving E at a transition rate σ , which is the reciprocal of the latent period. For the infectious cases, we model a proportion q of cases are asymptomatic (A), where q is the asymptomatic ratio, and thus $(1 - q)$ of cases are symptomatic (I). Eventually, all cases in A and I will either recover or die (and no longer infectious) at a transition rate γ , which is the reciprocal of the infectious period. Hence, there are 2 transition pathways ' $S \rightarrow E \rightarrow A \rightarrow R$ ' and ' $S \rightarrow E \rightarrow I \rightarrow R$ ' considered.

For the term β , we consider the same effective contact rate for the asymptomatic and symptomatic cases merely for simplicity. Complex scenarios can be extended by considering different transmission characteristics of asymptomatic and symptomatic cases, e.g., an asymptomatic case is partially infectious as a symptomatic case by a constant factor. In addition, the pre-symptomatic transmission period is considered as a part of infectious period (γ^{-1}), and thus the precise interpretation of I is the individuals who (may not yet but) develop symptoms eventually. Alternatively, a separated pre-symptomatic compartment can be modelled to consider this issue, which complicates the formulation. Note that

when the latent period approaches the incubation period, the pre-symptomatic transmission period will vanish. We remark that the simple settings adopted here will not change our conclusion.

2.1.2. Different epidemiological characteristics of mutated variants

For the cases, i.e., those in E , A , or I classes, we consider 2 types of variants as the pathogen of disease that are indicated by subscript '1' for the original variant, and '2' for the newly emerged (mutated) variant. Comparing against the original type, we consider several epidemiological characteristics of mutated variants that are different from the original. They include.

- a change in the effective contact rate, or transmission rate, (β) by a factor η_β ,
- a change in the asymptomatic ratio (q) by a factor η_q , and
- a change in the infectious period (γ^{-1}) by a factor η_γ .

All these 3 factors are positive (>0). Specially, for the range of η_q , it is subject to the condition that $0 \leq \eta_q q \leq 1$, such that the epidemiological meaning of asymptomatic ratio holds.

For interpretation, the factor η_β is the relative ratio of contagion (or infectivity) for the second type (new) against first type (original) of variants. The factor η_q is the relative ratio of being asymptomatic for the second type against first type of variants. The $1/\eta_\gamma$ is the relative ratio of recovery or death for the second type against first type of variants. In other words, the new variants prolong (or shorten) the infectious period by the factor η_γ . When any factor equals to 1, the corresponding epidemiological parameters are indifferent for the 2 types of variants.

The differences in these epidemiological characteristics were reported in literature among different SARS-CoV-2 variants for infectivity (Hui et al., 2022; Khan et al., 2021; Frampton et al., 2021), clinical severity or asymptomatic ratio (Loconsole et al., 2021), and time interval between transmission generations (Hart et al., 2022; Backer et al., 2022; Ong et al., 2021), as well as other features not included in the modelling study.

2.1.3. Compartmental model

We formulate the two-strain epidemic model as an ordinary differential equation (ODE) system expressed in Eqn. (1).

$$\begin{aligned}
 \frac{dS}{dt} &= -\beta S \cdot \frac{[(A_1 + I_1) + \eta_\beta \cdot (A_2 + I_2)]}{N}, \\
 \frac{dE_1}{dt} &= -\beta S \cdot \frac{(A_1 + I_1)}{N} - \sigma E_1, \\
 \frac{dE_2}{dt} &= -\eta_\beta \beta S \cdot \frac{(A_2 + I_2)}{N} - \sigma E_2, \\
 \frac{dA_1}{dt} &= q\sigma E_1 - \gamma A_1, \\
 \frac{dA_2}{dt} &= \eta_q q \sigma E_2 - \frac{\gamma}{\eta_\gamma} A_2, \\
 \frac{dI_1}{dt} &= (1 - q)\sigma E_1 - \gamma I_1, \\
 \frac{dI_2}{dt} &= (1 - \eta_q q)\sigma E_2 - \frac{\gamma}{\eta_\gamma} I_2, \\
 \frac{dR}{dt} &= \gamma \cdot \left[(A_1 + I_1) + \frac{(A_2 + I_2)}{\eta_\gamma} \right]
 \end{aligned} \tag{1}$$

Straightforwardly, for the total population $N = S + E_1 + E_2 + A_1 + A_2 + I_1 + I_2 + R$, we have $\frac{dN}{dt} = 0$, and thus, N is a constant. The daily numbers of new cases are formulated as $c_1(t) = \int_{dayt} \sigma E_1 dt$ for the original variant, and $c_2(t) = \int_{dayt} \sigma E_2 dt$ for the new variant. Hence, the overall daily number of new cases is $c(t) = c_1(t) + c_2(t)$.

This basic but elegant model includes several simplifying assumptions, such as exponential distributions of both latent and infectious periods, homogeneous mixing and long-lasting immunity after recovery. For convenience, we ignore the cases of co-infection, which were rarely reported, and re-infection, which occurs at a low rate with a long gap between two infections, by another variants. Since the infection fatality ratio of COVID-19 is relatively low, which is estimated from 0.7% to 1.3% among all SARS-CoV-2 infections (Russell et al., 2020; Verity et al., 2020), we assume all infections will eventually recovery for simplicity. The natural birth and death of human are also neglected since the effects of them are minor comparing to the transmission dynamics of COVID-19. Considering the ‘trade-off’ between the transmission rate (infectivity) and disease-induced death rate (virulence) (Acevedo et al., 2019), different infection fatality ratio can be further considered by setting additional ratio parameters to class R , which was omitted in this study. Although some of the assumptions are probably ‘unrealistic’, the system in Eqn. (1) provides a parsimonious approximation of the reality, which allows us to capture and investigate the general patterns and dynamics of COVID-19 epidemics.

2.2. Reproduction number

By definition, the reproduction number is the expected number of cases directly generated by one typical case in a population. As a well-studied metric that considers both reproducibility and survivability of the seed case, reproduction number is typically adopted to measure the fitness of a pathogen in maintaining its transmission (Metz et al., 1992; Diekmann et al., 2010; Schreiber et al., 2021).

At the disease-free equilibrium, with a wholly susceptible population, the basic reproduction numbers, denoted by \mathcal{R} , can be formulated by using the next generation matrix approach (van den Driessche and Watmough, 2002). For the first type of (i.e., original) strains, $\mathcal{R}_1^{(A)} = \frac{\beta}{\gamma}$ contributed by a typical asymptomatic case, i.e., A_1 , and $\mathcal{R}_1^{(I)} = \frac{\beta}{\gamma}$ contributed by a typical symptomatic case, i.e., I_1 . For the second type of (i.e., new) strains, $\mathcal{R}_2^{(A)} = \eta_\beta \eta_\gamma \cdot \frac{\beta}{\gamma}$ contributed by a typical asymptomatic case, i.e., A_2 , and $\mathcal{R}_2^{(I)} = \eta_\beta \eta_\gamma \cdot \frac{\beta}{\gamma}$ contributed by a typical symptomatic case, i.e., I_2 . Apparently, $\mathcal{R}_1^{(A)} = \mathcal{R}_1^{(I)}$ and $\mathcal{R}_2^{(A)} = \mathcal{R}_2^{(I)}$, and this is merely because we have assumed the same profiles for asymptomatic and symptomatic cases for simplicity. We remark that assuming different profiles for asymptomatic and symptomatic cases will not affect our main conclusions.

Combining the 2 parts, we have $\mathcal{R}_1 = q\mathcal{R}_1^{(A)} + (1-q)\mathcal{R}_1^{(I)} = \frac{\beta}{\gamma}$ and $\mathcal{R}_2 = \eta_q q\mathcal{R}_2^{(A)} + (1-\eta_q q)\mathcal{R}_2^{(I)} = \eta_\beta \eta_\gamma \cdot \frac{\beta}{\gamma}$. Considering the whole model, the basic reproduction number, denoted by \mathcal{R}_0 , is composed of \mathcal{R}_1 and \mathcal{R}_2 . We denote the probability that a case is infected by the first type of strain as p , and thus, $(1-p)$ for the second type of strain. Then, $\mathcal{R}_0 = p\mathcal{R}_1 + (1-p)\mathcal{R}_2$. From the epidemiological standpoint, the term p can be interpreted as the proportion of the first type of strains among the source of infection, or as the prevalence of the active cases who are infected by the first (original) type of strains. Straightforwardly, when the second (new) type of strain is absent, i.e., $p = 1$, the basic reproduction number becomes β/γ , which is equivalent to that of the classic susceptible-infectious-removed (‘SIR’) model.

By contrast to \mathcal{R}_0 , the effective reproduction number, denoted by \mathcal{R}_{eff} , is commonly adopted when accounting for the depletion of the susceptible population. We have $\mathcal{R}_{\text{eff}} = \mathcal{R}_0 \cdot \frac{S}{N}$, which is less than (or equal to) \mathcal{R}_0 by definition. Since S is time-varying during the course of an epidemic, \mathcal{R}_{eff} is also considered as a

time-varying metric. In an epidemic of infectious disease, non-pharmaceutical interventions are commonly implemented to mitigate the outbreak size. When the control measures are considered, the effective reproduction number will be reduced, which is sometimes referred to as the controlled reproduction number.

2.3. Transmission advantage

2.3.1. Intrinsic transmission advantage

For infectious disease, the transmission advantage (η) of a pathogen against another is typically quantified by the relative fitness. Thus, the term η is defined as the ratio between two reproduction numbers, which was adopted to study the epidemics of gonorrhoeae (Whittles et al., 2017), influenza (Leung et al., 2017), HIV (Kühnert et al., 2018), and COVID-19 (Zhao et al., 2021a; Volz et al., 2021a; Faria et al., 2021). As such, $\eta = \frac{\mathcal{R}_2}{\mathcal{R}_1} = \eta_\beta \eta_\gamma$ for the second type against the first type of strains in a general context. Note that the term η indicates the advantage of transmission under a natural selection-free context, namely the intrinsic transmission advantage.

Specifically, the transmission advantage (of the second against first type) is $\eta^{(A)} = \frac{\mathcal{R}_2^{(A)}}{\mathcal{R}_1^{(A)}} = \eta_\beta \eta_\gamma$ for the asymptomatic cases, and

$\eta^{(I)} = \frac{\mathcal{R}_2^{(I)}}{\mathcal{R}_1^{(I)}} = \eta_\beta \eta_\gamma$ for the symptomatic cases. Hence, we have $\eta = \eta^{(A)} = \eta^{(I)}$. Here, we consider the multiplicative transmission advantage, and alternatively, the transmission advantage might also be defined additively (Davies et al., 2021; Volz et al., 2021a; Volz et al., 2021b), which leads to similar conclusions and is not discussed in this study to avoid repeating.

2.3.2. Effective transmission advantage

Since the selection pressures contribute to alter the fitness, the intrinsic transmission advantage appears limited in more realistic contexts. We consider the situation that the non-pharmaceutical interventions (NPIs) are placed. The effective transmission advantage, denoted by η_{eff} , accounts for the effects of selection pressures from NPIs to the disease transmission, which is an extension of the concept of intrinsic transmission advantage. Thus, the η_{eff} is defined as the ratio between the effective reproduction numbers of the second type and first type of variants. Similar to the intrinsic transmission advantage, if $\eta_{\text{eff}} > 1$ the new variants are more transmissible than the original variants, the larger η_{eff} becomes the prevalence of new variants grows more rapidly, and *vice versa*.

In the remaining parts of this work, we demonstrate several scenarios that the effective transmission advantage may become time-varying when the NPIs are implemented during epidemics.

3. Numerical simulations

To illustrate the way how NPIs may affect the transmission advantage, we conduct the numerical simulations using the settings and schemes introduced in this section.

3.1. Settings and initialization

3.1.1. Fixed epidemiological parameters

Without losing the generality, we set the values for model parameters according to the epidemiological characteristics of the COVID-19 for demonstration. The mean latent period is considered at $\sigma^{-1} = 3.5$ days referring to the previous estimates at 3.3 days in (Zhao, 2020), and from 3.4 to 3.7 in (Li et al., 2020). The mean infectious period is set at $\gamma^{-1} = 4.0$ days, which is based on the previous calculations in (Wu et al., 2020; Li et al., 2020; Kucharski

et al., 2020; Read et al., 1829). We set asymptomatic ratio at $q = 30\%$ by choosing the middle point of the range from 20% to 40% estimated in (Roxby et al., 2020; Gudbjartsson et al., 2020; Mizumoto et al., 2020; Nishiura et al., 2020).

The total population is considered at $N = 1,000,000$ individuals. We consider the basic reproduction number for the first type of variants at $\mathcal{R}_1 = 2.2$, which is in line with most of existing estimates (Li et al., 2020; Wu et al., 2020; Du et al., 2020; Ferretti et al., 2020; Lin et al., 2020; Nishiura et al., 2019; Wang et al., 2020; Zhao et al., 2020; Ran et al., 2020). As such, the value of β can be calculated by using the formula $\mathcal{R}_1 = \frac{\beta}{\gamma}$ backwardly.

For the changing factors of the mutated (new) variants, i.e., η_β , η_q and η_γ , we consider values larger than 1 because the emerging variant usually appears more competitive than the original variants. For convenience, we assume $\eta_\beta = 1.2$, $\eta_q = 1.5$ and $\eta_\gamma = 2.0$ fixed for demonstration. Then, we have $\eta = \eta_\beta \eta_\gamma = 2.4$. Thus, the value of \mathcal{R}_2 can be calculated by using the relationship $\frac{\mathcal{R}_2}{\mathcal{R}_1} = \eta_\beta \eta_\gamma$, and we have $\mathcal{R}_2 = 5.28$. Note that in the real-world situation, the values of η_β , η_q and η_γ can be very different, and thus the assumed values in model situation are merely for illustration at a conceptual level, which not necessarily reflects the characteristics of SARS-CoV-2 variants. Other values may merely change the numerical results, but will not affect the main conclusions.

3.1.2. Initial conditions

Since it is the first outbreak of COVID-19 in human history, we assume the initial susceptible population with a relatively large scale, and at $S(t=0)/N = 99\%$ as of the start of simulation, i.e., $t = 0$. For the seed cases, we mimic the situation that the new variants start emerging from a low prevalence when the original variants circulate among individuals. As such, we consider 99 and 1 exposed cases infected the original (E_1) and new (E_2) variants at the initial stage, respectively. Thus, the prevalence of the new variant is $1\% (=1 - p)$ at the initial stage. The rest proportion (0.99%) of the population are all assigned to class R .

Using $\mathcal{R}_0 = p\mathcal{R}_1 + (1 - p)\mathcal{R}_2$, we calculate $\mathcal{R}_0 = 2.23$. With the initial conditions fixed, the initial $\mathcal{R}_{\text{eff}}(t=0) = \mathcal{R}_0 \cdot \frac{S(t=0)}{N} = 2.21$.

3.2. Simulation schemes for different non-pharmaceutical interventions

We consider and simulate 5 scenarios with (or without) the implementation of NPIs. For each scenario, we simulate the epidemic models based on Eqn. (1) deterministically for 120 days using the fix-time-step Euler's method with $dt = 1/365.25$ year, which is equivalent to 1 day on the scale of a year.

Under each scenario, we record the change in the model conditions due to NPIs, and extract the characteristics of transmission, including reproduction number and transmission advantage metrics, and key epidemiological outcomes, including the number of cases and proportion of each variant, from the simulation results.

3.2.1. Scenario (#0): Without non-pharmaceutical intervention

We consider the scenario (#0) that NPI is absent. As the baseline scenario, scenario (#0) is simulated and compared as the reference level for other scenarios with NPIs. In scenario (#0), the predefined model conditions are fixed such that both effective reproduction numbers of original and new variants only depend on the depletion of S simultaneously. Therefore, the effective transmission advantage $\eta_{\text{eff}} = \eta = 2.4$ also holds constant. Since NPIs are expected to mitigate the size of outbreak, the number of cases (c) in scenario (#0) is the upper bound of all scenarios.

3.2.2. Scenario (#1): reduction in infectivity by personal protective equipment

One of the major impacts of NPIs is to reduce the infectivity (i.e., transmission rate β) of the sources of infection, e.g., infectors, which can be achieved by, for instance, the adoption of personal protective equipment (PPE). For instance, facemask and hand sanitizer may significantly decrease the chance of respiratory infection (Cowling et al., 2009). To investigate the impacts of infectivity reduction on transmission advantage, a fractional reduction in the infectivity is modelled. For illustration, we reduced 30%, 50% and 70% of the infectivity of both original and new variants on day 40, 60 and 80, respectively. Here, we consider changes in infectivity due to PPE are unlikely sensitivity to genetic mutations, and thus infectivity of new variants is considered equally likely to be reduced by PPE than that of original variants under scenario (#1).

Alternatively, we relax the restriction in model conditions, and consider 2 additional sub-scenarios that infectivity of new variants is less or more likely to be reduced by PPE than that of original variants, which is presented in [Supplementary Information S1.1](#).

3.2.3. Scenario (#2): isolation of symptomatic cases

It is possible that a mutated (new) variant may potentially result in a set of clinical conditions (or symptoms) that appear different than those of the original variants. The differences in symptoms may result in different detection ratio, which also changes the isolation proportion since cases isolation (or self-isolation) is typically implemented immediately after detection by symptoms. We consider that a fraction (i.e., isolation proportion) of symptomatic cases is timely detected and then isolated. To mimic the effects of case isolation, we remove an isolation proportion of symptomatic cases directly to the recovery class (R). Note that the transition pathways for the asymptomatic cases remain unchanged, which means no isolation is applied for asymptomatic cases. For illustration, we remove 20%, 60% and 80% of the symptomatic cases infected by both original and new variants on day 40, 60 and 80, respectively.

We explore how the differences in the clinical conditions of variants and in the implementation of symptomatic case isolation shapes the profile of transmission advantage. Alternatively, we relax the restriction in model conditions, and consider 2 additional sub-scenarios that symptomatic cases of new variants are less or more likely to be detected than those of original variants, which is presented in [Supplementary Information S1.2](#).

3.2.4. Scenario (#3): early detection by contact tracing

Contact tracing is commonly implemented to find linked infected within transmission clusters. Under intensive contact tracing, cases can be detected timely (and followed by isolation) such that future transmission can be prevented. Here, we model the effect of early detection and isolation by directly removing the cases to the recovery class (R) immediately after detection. Specifically, we assume the mean detection delay, or containment delay (Du et al., 2020), at 3.5, 2.5 and 1.5 days on day 40, 60 and 80, respectively for illustration. Thus, if the mean infectious period is larger than the mean detection delay, the mean infectious period will be changed to the mean detection delay, which mimics the case isolation after detection. This applies to both asymptomatic and symptomatic cases.

3.2.5. Scenario (#4): enhancement of stay-at-home and social distancing

To avoid confusion, we re-visit the previous scenario (#1) for more clarification before introducing scenario (#4). In scenario (#1), the infectivity is reduced by proportionally decreasing the transmission rate β , which is considered as the effect from PPE. To clarify, we crudely decompose term β into the contact rate (de-

noted by b) and transmission probability per contact (denoted by α , and $0 \leq \alpha \leq 1$), and thus $\beta = \alpha b$ according to the classic epidemiological theory. Since the PPE will not affect the scale of term b , the reduction in infectivity under scenario (#1) is to reduce α , which also decrease β . Therefore, more specifically, the factor η_β controls the advantage in α .

In NPI-absence situation, the transmission occurs with a high b but a low α , which reflects the general contexts of public places including workspace, market, and school. However, with social distancing, people are forced to stay at private location such as hotel and private residence, which implies a low b but a high α . The α becomes higher because social distancing increases the duration and proximity of each contact. Under scenario (#4), although the product of αb decreases, the increase in α may lead to different changing patterns of transmission advantage. Indeed, the proportion of household infections becomes more common with intensive social distancing. Note that the value of α may become remarkably high, and even close to 1, under intensive social distancing, which means if infectors are almost certain to transmit disease to their close contacts.

For illustration, we firstly fix $\alpha = 0.5$ for the original variants at the initial stage of simulation (i.e., $t = 0$), and thus the value of b (for both original and new variants) can be calculated by using the initial settings in Section 3.1.1. For the new variant, we have $\eta_\beta \alpha = 0.6$. Then, we reduced 30%, 50% and 70% of b on day 40, 60 and 80, respectively, which models the impact of the social distancing on reducing the contact rate b . Note that, at this stage, the exact same simulation outcomes as those of scenario (#1) can be obtained because the same values of β series are also assigned here. Next, we model that social distancing leads to increase in transmission probability per contact α . We consider increase in α with factors 1.2, 1.5 and 2.0 on day 40, 60 and 80, respectively. To check the overall effect, we have $(1 - 30\%) \times 1.2 = 84\%$, $(1 - 50\%) \times 1.5 = 75\%$ and $(1 - 70\%) \times 2.0 = 60\%$ as the changing factor for β , which mimics the overall decreasing trends for the transmission rate due to social distancing. Note that the value of transmission probability per contact will be restricted at 1 when exceeding.

Equivalently, the impacts of social distancing in α and b can be explicated modelled by decompose the transmission rate into 2 additive parts including public-space and household transmission. Then, we have $\beta_1 = \alpha_p b_p + \alpha_h b_h$ for original strains, and $\beta_2 = \eta_\beta (\alpha_p b_p + \alpha_h b_h)$, where the subscript 'p' and 'h' denotes the public-space and household transmission setting, respectively. For the transmission probability per contact, we have $b_p < b_h < \eta_\beta b_h < 1$, which indicates household contact are more likely to be infected. For the attributed change in transmission rate without social distancing, it is $[\eta_\beta (\alpha_p b_p + \alpha_h b_h)] / (\alpha_p b_p + \alpha_h b_h) = \eta_\beta$ as pre-defined. With social distancing, we remove the contribution of public-space transmission ($\alpha_p b_p$) and increase the household transmission probability per contact (i.e., $b'_h > b_h$), and attributed change in transmission rate is $\min[\eta_\beta (\alpha_h b'_h), \alpha_h] / (\alpha_h b'_h) = (\eta_\beta b'_h) / b'_h = \min[\eta_\beta, 1/b'_h] \leq \eta_\beta$, where $\eta_\beta b'_h$ must not exceed 1. Hence, social distancing might lead to a decrease in transmission advantage due to a saturation in household transmission probability per contact. Although this explicit decomposition of public-space and household transmission was not adopted for simulation here, we remark that similar numerical outcomes can be reached, which leads to the same conclusion.

4. Results

Considering the effects of PPE under scenario (#1), although the reduction in infectivity can be achieved in terms of the effective reproduction number (R_{eff}) and flattening the epidemic curve

(comparing to the outcome without NPI, i.e., baseline scenario), the transmission advantage (η_{eff}) holds unchanged, see Fig. 1. Since the reduced infectivity of new or original variants in scenario (#1) are always proportional to each other, and thus the value of η_{eff} appears unchanged. The prevalence of new variants almost follows the same pattern as that without NPI. The outcomes appear different if the infectivity of new variants is not equally (i.e., more, or less) likely to be reduced than that of original variants. We find η_{eff} may increase when the infectivity of new variants is less likely to be reduced (i.e., insensitive to PPE), but η_{eff} may decrease and even become lose effect (i.e., < 1 , theoretically but unrealistic) otherwise, see Supplementary Information S1.1. Practically, the 2 types of variants are more likely to be equally sensitive to the PPE, and thus the unchanged η_{eff} in Fig. 1 is included as the main results. Many existing studies follow the context of scenario (#1) (Leung et al., 2021; Zhao et al., 2021a; Davies et al., 2021; Faria et al., 2021; Volz et al., 2021b), where the transmission advantage is considered as a constant regardless of the change in reproduction number.

Another important and efficient NPI is the isolation of individuals with symptoms matching clinical conditions of COVID-19 (e.g., high body temperature, sore throat, and headache), namely isolation of symptomatic cases in scenario (#2). Since a fraction of cases are isolated and thus cannot contribute to the transmission, the R_{eff} decreases and the epidemic curve is flattened, see Fig. 2. However, the η_{eff} increases when more fraction of symptomatic cases are isolated. We also find that the prevalence of the new variant increases faster than the scenario without NPI, see Fig. 2G. If the isolation proportion for symptomatic case becomes extremely high (e.g., 100% isolation), the value of effective transmission advantage will approach the product of $\eta_\beta \eta_q \eta_\gamma$. This means the transmission advantage governed by the asymptomatic ratio (η_q) can be traded by eliminating the transmissibility of symptomatic cases. By contrast, if $\eta_q < 1$, the η_{eff} may decrease when more fraction of the symptomatic cases are isolated. The outcomes appear different if the symptomatic cases of new variants are not equally (i.e., more, or less) likely to be isolated than those of original variants. We find that the η_{eff} is decreased or increased dynamically depending on the different proportion of symptomatic cases isolation for the 2 types of variants, see Supplementary Information S1.2. However, it appears that the genetic mutations in pathogen seldomly cause any distinguishable (and detectable) difference in clinical conditions (Graham et al., 2021), and thus symptomatic cases of new variants are equally likely to be detected (and thus isolated) than those of original variants under the scenario (#2).

Contact tracing is frequently implemented to find individuals with high risk of exposure, and prevent future transmission, see scenario (#3). Since all cases under intensive contact tracing will be detected earlier and isolated, the R_{eff} decreases and the size of outbreak is reduced, see Fig. 3. However, the η_{eff} decreases when the contact tracing is implemented. Here, we consider a simplified assumption that the contact tracing reduces the infectious periods of both variants to the same value, which matches the findings in containment delay (Du et al., 2020; Kwok et al., 2021; Ran et al., 2020). In other words, each case is expected to be detected and isolated certain period (e.g., 3.5, 2.5 and 1.5 days used in section 3.2.4) after latency. Once the infectious periods for both original and new variants appear the same, and thus the (part of) transmission advantage governed by factor η_γ vanishes. Thus, the value of η_{eff} decreases from $\eta_\beta \eta_\gamma = 2.4$ to $\eta_\beta = 1.2$ as we set, see Fig. 3C. It worth noting that due to the dramatical change in η_{eff} , the growth of the proportion of new variants is evidently slowed, see Fig. 3G, which indicates the contact tracing may delay the new variant reaching dominance in the population.

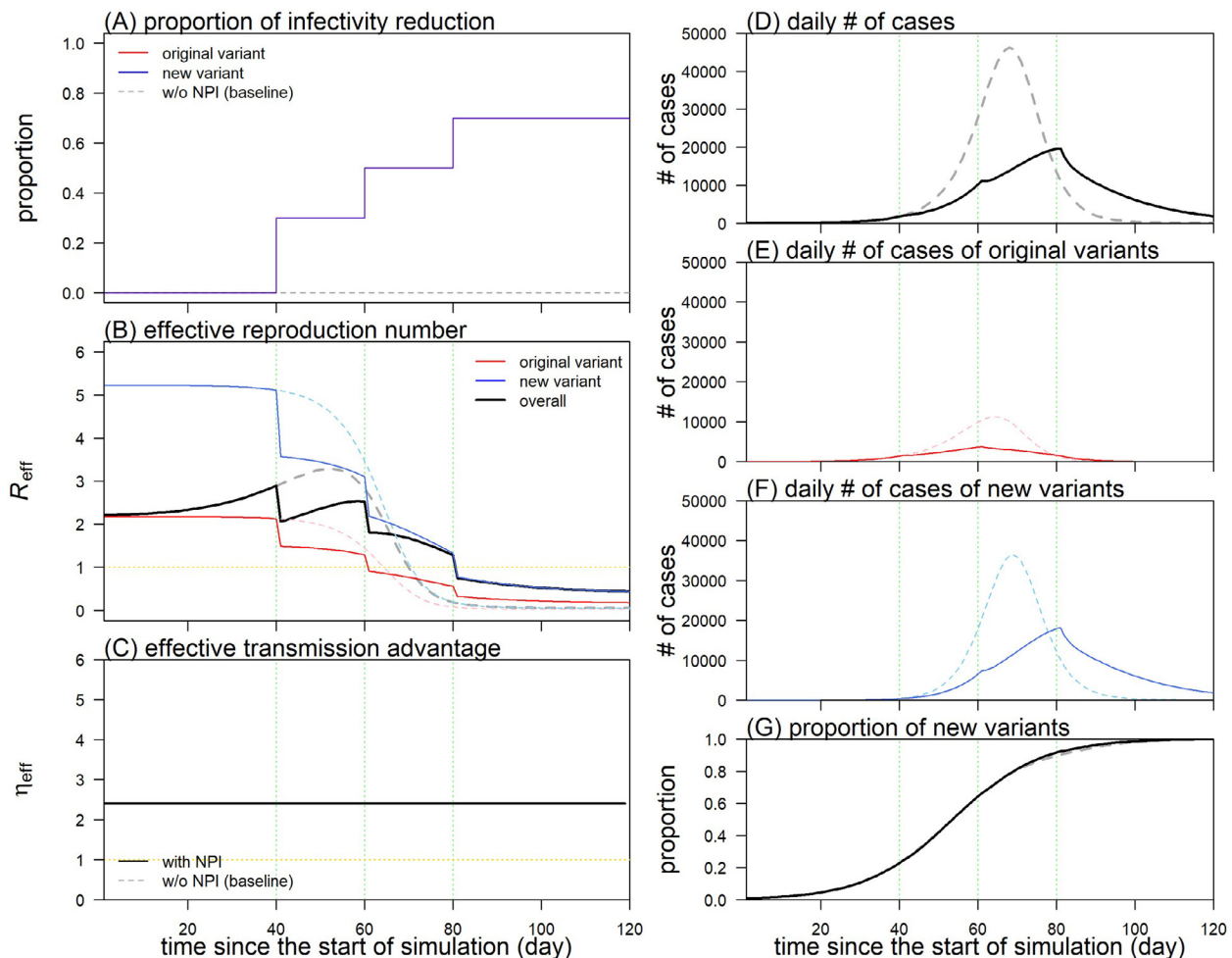


Fig. 1. The simulation results of scenario (#1), reduction in infectivity by personal protective equipment (PPE). In panel (A), the infectivity (β) of both original and new variants is reduced by 30%, 50% and 70% on day 40, 60 and 80, respectively. Panels (B) and (C) show the changing patterns of effective reproduction number (R_{eff}) and effect transmission advantage (η_{eff}), respectively. Panels from (D) to (F) present the daily number of new cases infected by both, original, and new variants, respectively. Panel (G) shows the changing patterns of the new variants' prevalence. In all panels, the scenario with NPIs and the baseline scenario (#0) without NPIs are indicated by the normal (original variants in red and new variants in blue) and dashed curves, respectively. The vertical green dashed lines indicate the timing when NPIs in panel (A) are implemented.

The social distancing appears one of the commonly adopted NPI against COVID-19 pandemic (Teslya et al., 2020). In scenario (#4), we highlight the increase in transmission probability per contact α despite the reduction in contact rate b as well as the overall reduction in transmission rate β , which is thus distinguished from scenario (#1). In Fig. 4, the number of cases is decreased due to the impacts of social distancing. The η_{eff} also decreases in Fig. 4C when the term α of both variants reaching 1 in Fig. 4A. Namely, contacts who are closely connected to the source of infection (i.e., infector) are highly likely to become infected, which occurs frequently at private places. As α increasing and reaching 1, β of the 2 types of variants approaches each other and eventually converges to the same value. Thus, η_{eff} decreases from $\eta_{\beta}\eta_{\gamma}$ to η_{γ} , which indicates the transmission advantage controlled by the factor η_{β} vanishes.

5. Discussion

In this study, we demonstrated that NPIs can not only control the intensity of epidemics, but also slow or even contain the growth of mutated variants' proportion through changing the transmission advantage. In the context of disease transmission,

the reproduction number (R_{eff}) determined both cases time series and epidemic size, and strain-specific reproduction numbers determined the transmission advantage of each strain. NPIs may change the reproduction numbers of different strains to different levels, and thus both epidemic curve and transmission advantage may be altered, see the summary in Table 1. Moreover, the change in transmission advantage due to NPIs (or sometimes not) also affects the process of viral variants establishing their dominance at the population scale through transmission. Our modelling framework conceptualized the impacts and mechanisms of (different types of) NPIs on the dynamics of transmission for different virus strains, which may further lead to a change in the selection advantage among strains.

In the practice, various types of NPIs are usually implemented simultaneously to achieve a mixed impact on disease control at populational scale. As one of typical NPIs, social distancing in scenario (#4) is commonly implemented together with recommendation of PPE in scenario (#1). As we elaborated in section 3.2.5, PPE aims at reducing α , and social distancing aims at reducing contact rate b but could rise α unexpectedly. The combined effects of PPE and social distancing on term α might offset to some (unknown) degree by each other, see Figs. 1A and 4A. As such, the decrease

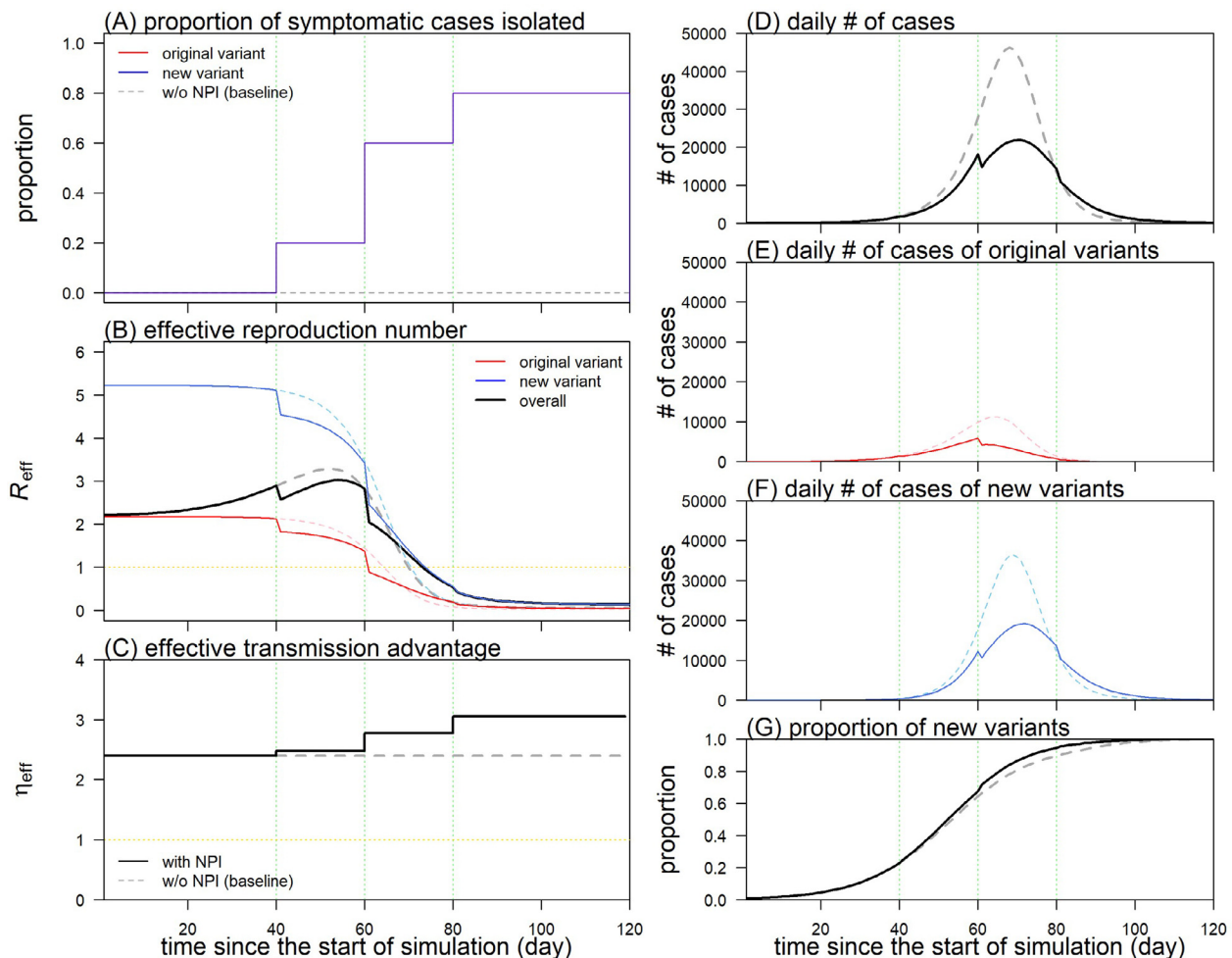


Fig. 2. The simulation results of scenario (#2), isolation of symptomatic cases. In panel (A), 20%, 60% and 80% of the symptomatic cases infected by both original and new variants are detected and immediate isolated on day 40, 60 and 80, respectively. Panels (B) and (C) show the changing patterns of effective reproduction number (R_{eff}) and effect transmission advantage (η_{eff}), respectively. Panels from (D) to (F) present the daily number of new cases infected by both, original, and new variants, respectively. Panel (G) shows the changing patterns of the new variants' prevalence. In all panels, the scenario with NPIs and the baseline scenario (#0) without NPIs are indicated by the normal (original variants in red and new variants in blue) and dashed curves, respectively. The vertical green dashed lines indicate the timing when NPIs in panel (A) are implemented.

in η_{eff} owing to social distancing might become minor when the PPEs are also adopted. However, under intensive social distancing measures, e.g., national or regional level restrictions, the increase in α may dominant against the decreasing effect of PPE. For instance, the decline in the effective transmission advantage of B.1.1.7 SARS-CoV-2 lineage, which was found in (Volz et al., 2021a), coincides with enforced social distancing and (Tier 3 and Tier 4) local restrictions in England since December 2020 (Graham et al., 2021).

Considering the symptomatic case isolation under scenario (#2), the changes in η_{eff} are also determined by the setting of η_q . In the real-world situation, the impact of symptomatic case isolation vanishes if the asymptomatic ratios (q) are the same for both variants (Graham et al., 2021), which means η_{eff} holds unchanged with $\eta_q = 1$. Under scenario (#3), contact tracing may contribute to change η_{eff} when $\eta_\gamma \neq 1$. However, we detect no evidence about the change in infectious period (γ^{-1}) attribute to the genetic mutation, and the value of η_γ is probably around 1. Thus, little impact on η_{eff} from contact tracing could occur.

In all scenarios, the epidemics are controlled considering the number of cases, peaking size, and the decay time of peak, which

reflects the effectiveness of NPIs. The key impacts of each type of NPI on the epidemiological parameters and effective transmission advantage are summarized qualitatively in Table 1. By affecting η_{eff} , the growing patterns of the proportion of new variants, denoted by $\rho(t) = \frac{c_2(t)}{c(t)}$, are also changed to some extent. We further note that large and early decrease in η_{eff} could cause that the trend of $\rho(t)$ becomes dramatically slower than the baseline scenario. For example, a large drop in η_{eff} before the new variants reach dominance, i.e., proportion $\rho(t) < 50\%$, due to timely NPIs (Fig. 3C) may lead to an evident change in $\rho(t)$, see Fig. 3G.

Besides the 3 factors η_β , η_q , and η_γ controlling the difference in epidemiological characteristics attributed to mutations, see section 2.1.2, the real-world biological impacts of mutation are probably more complex. We consider that the 3 factors formulated in Eqn. (1) represent the simplified but most likely scenarios that could occur. Other possible biological mechanisms that may induce transmission advantage include immune escape (i.e., risk of re-infection), increasing susceptibility in a group of population, and decreasing fatality risk so that the infector has a chance to transmit to more individuals, which are partially discussed in (Davies et al., 2021). Although many intrinsic features of mutated variants could

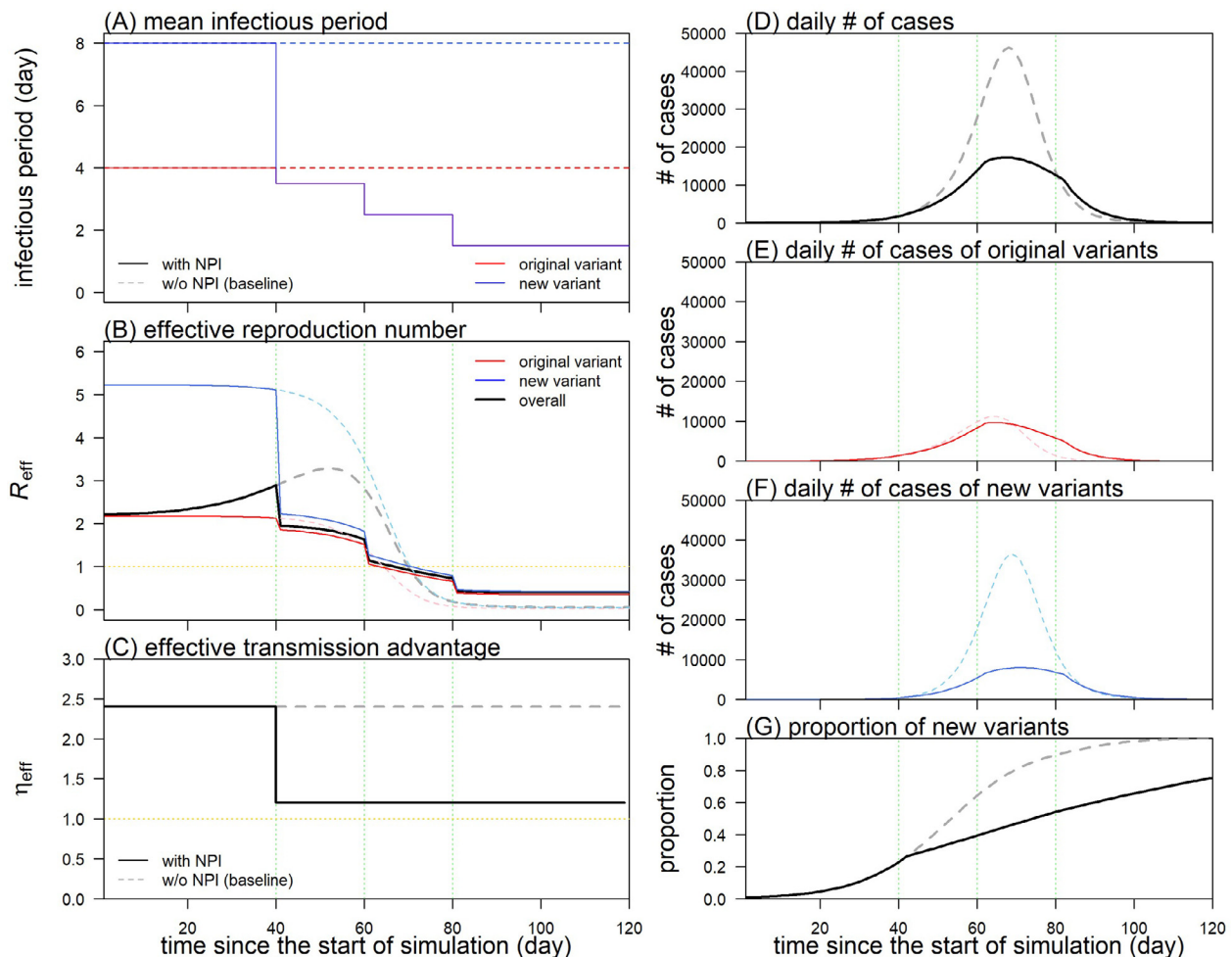


Fig. 3. The simulation results of scenario (#3), early detection by contact tracing. In panel (A), the mean infectious periods (equivalently, detection delay, or containment delay) of both variants are reduced at 3.5, 2.5 and 1.5 days on day 40, 60 and 80, respectively. Panels (B) and (C) show the changing patterns of effective reproduction number (R_{eff}) and effect transmission advantage (η_{eff}), respectively. Panels from (D) to (F) present the daily number of new cases infected by both, original, and new variants, respectively. Panel (G) shows the changing patterns of the new variants' prevalence. In all panels, the scenario with NPIs and the baseline scenario (#0) without NPIs are indicated by the normal (original variants in red and new variants in blue) and dashed curves, respectively. The vertical green dashed lines indicate the timing when NPIs in panel (A) are implemented.

bring mixed contributions to the viral fitness, the impacts of η_β , η_q , and η_γ , especially η_β , are the most commonly considered scenarios in many studies of COVID-19 (Leung et al., 2021; Zhao et al., 2021a; Faria et al., 2021), and influenza (Leung et al., 2017; Gog et al., 2003), which are more likely the dominant factors shaping the transmission advantage.

In scenarios (#1), (#2) and (#4), the impacts of NPIs are simulated by changing the epidemiological parameters in Eqn. (1) multiplicatively. Since the transmission advantage (η or η_{eff}) is defined as a multiplicative factor between reproduction numbers, see section 2.3, we consider that the multiplicative changes in the parameters provide a 'fair' comparison of the η_{eff} before and after the implementation of various NPIs. Alternatively, additive changes can be adopted to mimic the impacts of NPI. We note that the additive changes in parameters are more likely to result in the changes of η_{eff} , consider section 3.2.4 as an example. Regardless of the additive or multiplicative changes, we demonstrated that NPI may lead to change in the transmission advantage (η_{eff}) that appears differently from its intrinsic value (η), which is likely to occur when the level of NPIs becomes intensive.

For the limitations of this study, we merely demonstrated how NPI changes over time may lead to the change in transmission advantage. We discuss that the spatial heterogeneity in the implementation of NPIs may also cause and amplify the difference in transmission advantage. For example, the transmission advantage of B.1.1.7 SARS-CoV-2 lineage appears at different scales in different regions of England (Graham et al., 2021), and in other places (Davies et al., 2021; Zhao et al., 2022). Aside from NPIs, other non-pharmaceutical factors, e.g., weather and pollutants, might affect the infectivity to different degrees regarding different variants. For example, although lack real-world supportive evidence, the mutations might alter the viability of viruses that become more adaptive to warm weather, which implies the changes in infectivity are different for the original and new variants as temperature increases. Recent study also reported that the transmission advantage of B.1.1.7 SARS-CoV-2 lineage appears (slightly) less than average for target individuals with ages from 10 to 30 years (Davies et al., 2021). As such, the NPIs having heterogeneous effects for different age groups could also lead to changes in transmission advantage. Although vaccine and other pharmaceutical

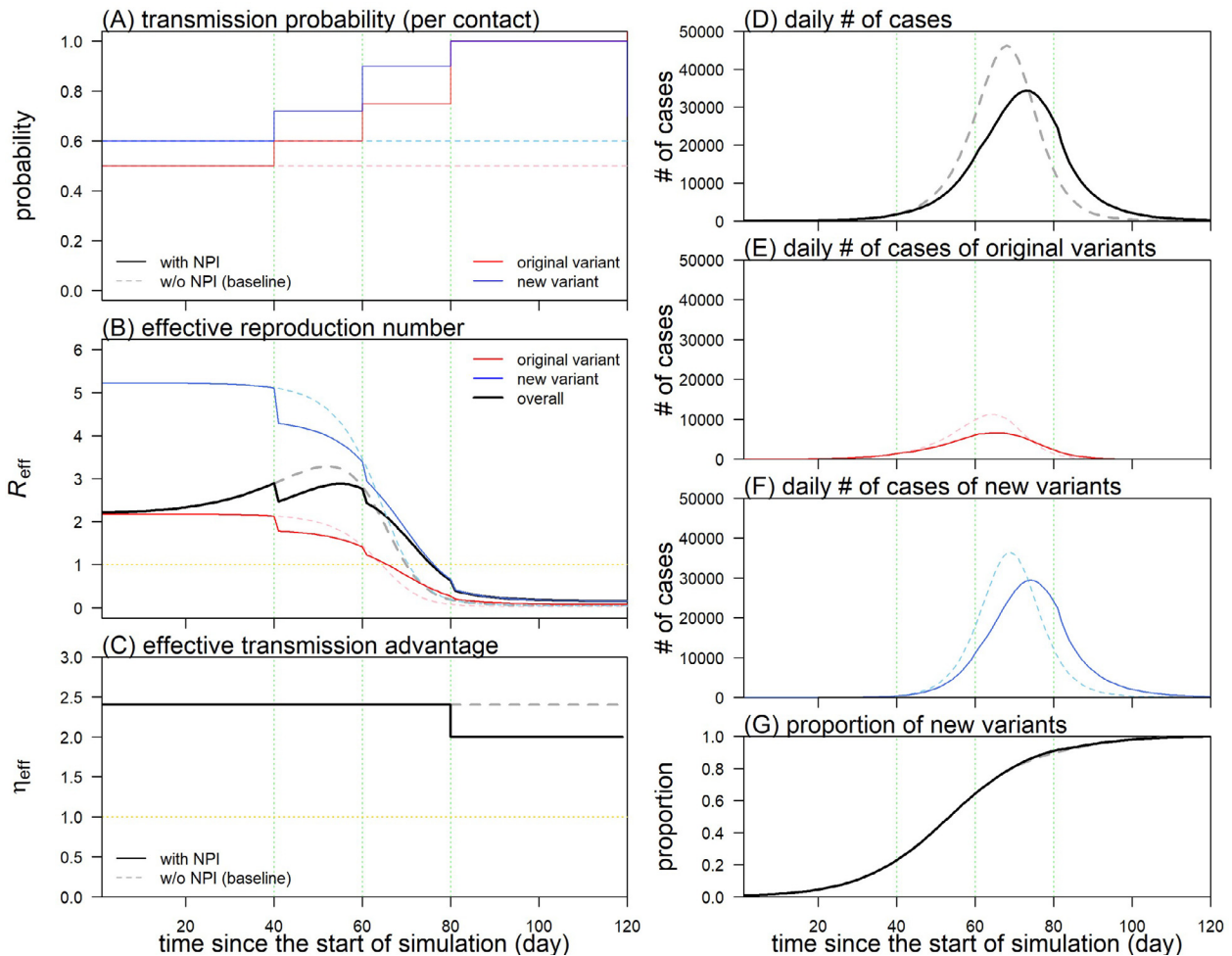


Fig. 4. The simulation results of scenario (#4), social distancing. In panel (A), the transmission probability per contact (α) gradually increases with factors 1.2, 1.5 and 2.0 on day 40, 60 and 80, respectively due to the enhancement of social distancing. Panels (B) and (C) show the changing patterns of effective reproduction number (R_{eff}) and effect transmission advantage (η_{eff}), respectively. Panels from (D) to (F) present the daily number of new cases infected by both, original, and new variants, respectively. Panel (G) shows the changing patterns of the new variants' prevalence. In all panels, the scenario with NPIs and the baseline scenario (#0) without NPIs are indicated by the normal (original variants in red and new variants in blue) and dashed curves, respectively. The vertical green dashed lines indicate the timing when NPIs in panel (A) are implemented.

Table 1
Qualitative summary on the key impacts of each type of NPI on the epidemiological parameters and effective transmission advantage.

scenario	in this study	type of NPI	impacts on	
			parameters or transmission dynamics	transmission advantage
(#0)	section 3.2.1	without NPI (baseline)	no change	no change
(#1)	section 3.2.2, Fig. 1	personal protective equipment	a reduction in infectivity with decreasing transmission probability per contact	may not change in reality
(#2)	section 3.2.3, Fig. 2	symptomatic cases isolation	a fraction of symptomatic cases are isolated, and thus their contribution to transmission vanishes	depending on η_q , and may change in reality
(#3)	section 3.2.4, Fig. 3	contact tracing	the containment delay is shortened	depending on η_r , and may decrease in reality
(#4)	section 3.2.5, Fig. 4	social distancing	reduction in infectivity with combined effects from decreasing contact rate but increasing transmission probability per contact	depending on η_p , and may decrease in reality

measures in controlling or treating an infectious disease may affect the selection advantage of different genetic variants of the pathogen at various scales, we concentrated on the impacts of NPIs in this study, and left these possible scenarios with both pharmaceutical and non-pharmaceutical interventions for future investigations.

6. Ethics approval and consent to participate

The ethical approval or individual consent was not applicable. The authors are accountable for all aspects of the work in ensuring that questions related to the accuracy or integrity of any part of the work are appropriately investigated and resolved.

7. Data availability statement

No real-world data is used in this work.

Funding

DH was supported by General Research Fund [15205119, and C7123-20G] of the Research Grants Council (RGC) of Hong Kong, China. MHW is supported by CUHK grant [PIEF/Ph2/COVID/06, and 4054456], the Health and Medical Research Fund (HMRF) Commissioned Research on COVID-19 [INF-CUHK-1] of Hong Kong, China, and partially supported by the National Natural Science Foundation of China (NSFC) [31871340, and 71974165].

CRediT authorship contribution statement

Shi Zhao: Conceptualization, Methodology, Software, Validation, Formal analysis, Investigation, Resources, Data curation, Writing – original draft, Visualization, Project administration. **Kai Wang:** Writing – review & editing. **Marc K.C. Chong:** Writing – review & editing. **Salihu S. Musa:** Writing – review & editing. **Mu He:** Writing – review & editing. **Lefei Han:** Writing – review & editing. **Daihai He:** Methodology, Writing – review & editing, Funding acquisition. **Maggie H. Wang:** Writing – review & editing, Supervision, Funding acquisition.

Declaration of Competing Interest

The authors declare the following financial interests/personal relationships which may be considered as potential competing interests: MHW is a shareholder of Beth Bioinformatics Co., Ltd. Other authors declared no competing interests. The funding agencies had no role in the design and conduct of the study; collection, management, analysis, and interpretation of the data; preparation, review, or approval of the manuscript; or decision to submit the manuscript for publication.

Acknowledgements

We acknowledge the helpful comments by professor D Gao from Shanghai Normal University, Shanghai, China at the early stage of this manuscript.

Appendix A. Supplementary data

Supplementary data to this article can be found online at <https://doi.org/10.1016/j.jtbi.2022.111105>.

References

- Acevedo, M.A., Dilleymuth, F.P., Flick, A.J., Faldyn, M.J., Elder, B.D., 2019. Virulence-driven trade-offs in disease transmission: a meta-analysis*. *Evolution* 73 (4), 636–647.
- Backer J.A., Eggink D., Andeweg S.P., Veldhuijzen I.K., van Maarseveen N., Vermaas K., Vlaemyck B., Schepers R., van den Hof S., Reusken C.B. et al: Shorter serial intervals in SARS-CoV-2 cases with Omicron BA.1 variant compared with Delta variant, the Netherlands, 13 to 26 December 2021. 2022, 27(6):2200042.
- Baum, A., Fulton, B.O., Wloga, E., Copin, R., Pascal, K.E., Russo, V., Giordano, S., Lanza, K., Negron, N., Ni, M., et al., 2020. Antibody cocktail to SARS-CoV-2 spike protein prevents rapid mutational escape seen with individual antibodies. *Science* 369 (6506), 1014–1018.
- Claro, I.M., da Silva Sales, F.C., Ramundo, M.S., Candido, D.S., Silva, C.A.M., de Jesus, J. G., Manuli, E.R., de Oliveira, C.M., Scarpelli, L., Campana, G., et al., 2021. Local transmission of SARS-CoV-2 Lineage B.1.1.7, Brazil, December 2020. *Emerg. Infect. Dis.* 27 (3), 970–972.
- Cowling, B.J., Chan, K.-H., Fang, V.J., Cheng, C.K.Y., Fung, R.O.P., Wai, W., Sin, J., Seto, W.H., Yung, R., Chu, D.W., et al., 2009. Facemasks and hand hygiene to prevent influenza transmission in households: a cluster randomized trial. *Ann. Inter. Med.* 151 (7), 437.

- Davies, N.G., Abbott, S., Barnard, R.C., Jarvis, C.I., Kucharski, A.J., Munday, J.D., Pearson, C.A.B., Russell, T.W., Tully, D.C., Washburne, A.D., et al., 2021. Estimated transmissibility and impact of SARS-CoV-2 lineage B.1.1.7 in England. *Science* 372 (6538).
- Diekmann, O., Heesterbeek, J.A.P., Roberts, M.G., 2010. The construction of next-generation matrices for compartmental epidemic models. *J. R. Soc. Interface* 7 (47), 873–885.
- Du, Z., Xu, X., Wu, Y., Wang, L., Cowling, B.J., Meyers, L.A., 2020. Serial Interval of COVID-19 among publicly reported confirmed cases. *Emerg. Infect. Dis.* 26 (6), 1341–1343.
- Du, Z., Xu, X., Wang, L., Fox, S.J., Cowling, B.J., Galvani, A.P., Meyers, L.A., 2020. Effects of proactive social distancing on COVID-19 outbreaks in 58 cities, China. *Emerg. Infect. Dis.* 26 (9), 2267–2269.
- Public Health England, Variants: distribution of cases data: Variants of concern or under investigation: data up to 7 April 2021 [<https://www.gov.uk/government/publications/covid-19-variants-genomically-confirmed-cases-numbers/variants-distribution-of-cases-data>].
- Faria, N.R., Mellan, T.A., Whittaker, C., Claro, I.M., Candido, D.d.S., Mishra, S., Crispim, M.A.E., Sales, F.C.S., Hawryluk, I., McCrone, J.T., 2021. Genomics and epidemiology of the P. 1 SARS-CoV-2 lineage in Manaus, Brazil. *Science* 372 (6544), 815–821.
- Ferretti, L., Wymant, C., Kendall, M., Zhao, L., Nurtay, A., Abeler-Dörner, L., Parker, M., Bonsall, D., Fraser, C., 2020. Quantifying SARS-CoV-2 transmission suggests epidemic control with digital contact tracing. *Science* 368 (6491).
- Frampton, D., Rampling, T., Cross, A., Bailey, H., Heaney, J., Byott, M., Scott, R., Sconza, R., Price, J., Margaritis, M., et al., 2021. Genomic characteristics and clinical effect of the emergent SARS-CoV-2 B.1.1.7 lineage in London, UK: a whole-genome sequencing and hospital-based cohort study. *Lancet Infect. Dis.* 21 (9), 1246–1256.
- Fraser, C., Riley, S., Anderson, R.M., Ferguson, N.M., 2004. Factors that make an infectious disease outbreak controllable. *Proc. Natl. Acad. Sci. USA* 101 (16), 6146–6151.
- Galloway, S.E., Paul, P., MacCannell, D.R., Johansson, M.A., Brooks, J.T., MacNeil, A., Slayton, R.B., Tong, S., Silk, B.J., Armstrong, G.L., 2021. Emergence of SARS-CoV-2 B.1.1.7 Lineage – United States, December 29, 2020–January 12, 2021. *MMWR Morb. Mortal. Wkly. Rep.* 70 (3), 95–99.
- Gog, J.R., Rimmelzwaan, G.F., Osterhaus, A.D.M.E., Grenfell, B.T., 2003. Population dynamics of rapid fixation in cytotoxic T lymphocyte escape mutants of influenza A. *Proc. Natl. Acad. Sci.* 100 (19), 11143–11147.
- Graham, M.S., Sudre, C.H., May, A., Antonelli, M., Murray, B., Varsavsky, T., Kläser, K., Canas, L.S., Molteni, E., Modat, M., 2021. Changes in symptomatology, reinfection, and transmissibility associated with the SARS-CoV-2 variant B. 1.1.7: an ecological study. *Lancet Public Health* 6 (5), e335–e345.
- Gudbjartsson, D.F., Norddahl, G.L., Melsted, P., Gunnarsdottir, K., Holm, H., Eythorsson, E., Arnthorsson, A.O., Helgason, D., Bjarnadottir, K., Ingvarsson, R. F., 2020. Humoral immune response to SARS-CoV-2 in Iceland. *N Engl J Med* 383 (18), 1724–1734.
- Hart, W.S., Miller, E., Andrews, N.J., Waight, P., Maini, P.K., Funk, S., Thompson, R.N., 2022. Generation time of the alpha and delta SARS-CoV-2 variants: an epidemiological analysis. *Lancet. Infect. Dis.*
- Hu, B., Guo, H., Zhou, P., Shi, Z.L., 2021. Characteristics of SARS-CoV-2 and COVID-19. *Nat. Rev. Microbiol.* 19 (3), 141–154.
- Hui, K.P.Y., Ho, J.C.W., Cheung, M.-C., Ng, K.-C., Ching, R.H.H., Lai, K.-I., Kam, T.T., Gu, H., Sit, K.-Y., Hsin, M.K.Y., et al., 2022. SARS-CoV-2 Omicron variant replication in human bronchus and lung ex vivo. *Nature*.
- Khan, A., Zia, T., Suleman, M., Khan, T., Ali, S.S., Abbasi, A.A., Mohammad, A., Wei, D.-Q., 2021. Higher infectivity of the SARS-CoV-2 new variants is associated with K417N/T, E484K, and N501Y mutants: An insight from structural data. *J. Cell Physiol.* 236 (10), 7045–7057.
- Kucharski, A.J., Russell, T.W., Diamond, C., Liu, Y., Edmunds, J., Funk, S., Eggo, R.M., 2020. Centre for Mathematical Modelling of Infectious Diseases C-wg: Early dynamics of transmission and control of COVID-19: a mathematical modelling study. *Lancet Infect. Dis.* 20 (5), 553–558.
- Kühnert, D., Kouyos, R., Shirreff, G., Pečerska, J., Scherrer, A.U., Böni, J., Yerly, S., Klimkait, T., Aubert, V., Günthard, H.F., 2018. Quantifying the fitness cost of HIV-1 drug resistance mutations through phylodynamics. *PLoS Pathog.* 14 (2), e1006895.
- Kutter, J.S., Spronken, M.I., Fraaij, P.L., Fouchier, R.A., Herfst, S., 2018. Transmission routes of respiratory viruses among humans. *Curr. Opin. Virol.* 28, 142–151.
- Kwok, K.O., Wei, W.I., Huang, Y., Kam, K.M., Chan, E.Y.Y., Riley, S., Chan, H.H.H., Hui, D.S.C., Wong, S.Y.S., Yeoh, E.K., 2021. Evolving epidemiological characteristics of COVID-19 in Hong Kong from January to August 2020: retrospective study. *J. Med. Internet Res.* 23 (4), e26645.
- Leung, K., Shum M.H., Leung G.M., Lam T.T., Wu J.T.: Early transmissibility assessment of the N501Y mutant strains of SARS-CoV-2 in the United Kingdom, October to November 2020. *Euro surveillance : bulletin Européen sur les maladies transmissibles = European communicable disease bulletin* 2021, 26 (1):2002106.
- Leung, K., Lipsitch, M., Yuen, K.Y., Wu, J.T., 2017. Monitoring the fitness of antiviral-resistant influenza strains during an epidemic: a mathematical modelling study. *Lancet. Infect. Dis.* 17 (3), 339–347.
- Li, Q., Guan, X., Wu, P., Wang, X., Zhou, L., Tong, Y., Ren, R., Leung, K.S.M., Lau, E.H.Y., Wong, J.Y., et al., 2020. Early Transmission Dynamics in Wuhan, China, of Novel Coronavirus-Infected Pneumonia. *N. Engl. J. Med.* 382 (13), 1199–1207.

- Li, R., Pei, S., Chen, B., Song, Y., Zhang, T., Yang, W., Shaman, J., 2020. Substantial undocumented infection facilitates the rapid dissemination of novel coronavirus (SARS-CoV-2). *Science* 368 (6490), 489–493.
- Lin, Y.-F., Duan, Q., Zhou, Y., Yuan, T., Li, P., Fitzpatrick, T., Fu, L., Feng, A., Luo, G., Zhan, Y., et al., 2020. Spread and Impact of COVID-19 in China: A Systematic Review and Synthesis of Predictions From Transmission-Dynamic Models. *Front. Med. (Lausanne)* 7.
- Loconsole D, Centrone F, Morcavallo C, Campanella S, Sallustio A, Accogli M, Fortunato F, Parisi A, Chironna M: Rapid Spread of the SARS-CoV-2 Variant of Concern 202012/01 in Southern Italy (December 2020–March 2021). 2021, 18 (9):4766
- Metz, J.A.J., Nisbet, R.M., Geritz, S.A.H., 1992. How should we define 'fitness' for general ecological scenarios? *Trends Ecol. Evol.* 7 (6), 198–202.
- Mizumoto K, Kagaya K, Zarebski A, Chowell G: Estimating the asymptomatic proportion of coronavirus disease 2019 (COVID-19) cases on board the Diamond Princess cruise ship, Yokohama, Japan, 2020. *Euro surveillance : bulletin Europeen sur les maladies transmissibles = European communicable disease bulletin* 2020, 25(10):2000180.
- Moore, J.P., Offit, P.A., 2021. SARS-CoV-2 Vaccines and the Growing Threat of Viral Variants. *JAMA* 325 (9), 821–822.
- Muik, A., Wallisch, A.-K., Sanger, B., Swanson, K.A., Muhl, J., Chen, W., Cai, H., Maurus, D., Sarkar, R., Tureci, ., et al., 2019. The Rate of Underascertainment of Novel Coronavirus (2019-nCoV) Infection: Estimation Using Japanese Passengers Data on Evacuation Flights. *J. Clin. Med.* 9 (2).
- Nishiura, H., Kobayashi, T., Yang, Y., Hayashi, K., Miyama, T., Kinoshita, R., Linton, N.M., Jung, S.M., Yuan, B., Suzuki, A., et al., 2019. The Rate of Underascertainment of Novel Coronavirus (2019-nCoV) Infection: Estimation Using Japanese Passengers Data on Evacuation Flights. *J. Clin. Med.* 9 (2).
- Nishiura, H., Kobayashi, T., Miyama, T., Suzuki, A., Jung, S.-M., Hayashi, K., Kinoshita, R., Yang, Y., Yuan, B., Akhmetzhanov, A.R., et al., 2020. Estimation of the asymptomatic ratio of novel coronavirus infections (COVID-19). *Int. J. Infect Dis.* 94, 154–155.
- Ong, S.W.X., Chiew, C.J., Ang, L.W., Mak, T.-M., Cui, L., Toh, M.P.H.S., Lim, Y.D., Lee, P.H., Lee, T.H., Chia, P.Y., et al., 2021. Clinical and Virological Features of Severe Acute Respiratory Syndrome Coronavirus 2 (SARS-CoV-2) Variants of Concern: A Retrospective Cohort Study Comparing B.1.1.7 (Alpha), B.1.351 (Beta), and B.1.617.2 (Delta). *Clin. Infect. Dis. ciab721*.
- Ran, J., Zhao, S., Han, L., Liao, G., Wang, K., Wang, M.H., He, D., 2020. A re-analysis in exploring the association between temperature and COVID-19 transmissibility: an ecological study with 154 Chinese cities. *Eur. Respir. J.* 56 (2), 2001253.
- Ran, J., Zhao, S., Zhuang, Z., Chong, M.K.C., Cai, Y., Cao, P., Wang, K., Lou, Y., Wang, W., Gao, D., 2020. Quantifying the improvement in confirmation efficiency of the severe acute respiratory syndrome coronavirus 2 (SARS-CoV-2) during the early phase of the outbreak in Hong Kong in 2020. *Int. J. Infect. Dis.* 96, 284–287.
- Read, J.M., Bridgen, J.R.E., Cummings, D.A.T., Ho, A., Jewell, C.P., 1829. Novel coronavirus 2019-nCoV (COVID-19): early estimation of epidemiological parameters and epidemic size estimates. *Philos. Trans. Royal Soc. B* 2021 (376), 20200265.
- Rondinone, V., Pace, L., Fasanella, A., Manzulli, V., Parisi, A., Capobianchi, M.R., Ostuni, A., Chironna, M., Caprioli, E., Labonia, M., et al., 2021. VOC 202012/01 Variant Is Effectively Neutralized by Antibodies Produced by Patients Infected before Its Diffusion in Italy. *Viruses-Basel* 13 (2), 276.
- Roxby, A.C., Greninger, A.L., Hatfield, K.M., Lynch, J.B., Dellit, T.H., James, A., Taylor, J., Page, L.C., Kimball, A., Arons, M.J.M., et al., 2020. Detection of SARS-CoV-2 Among Residents and Staff Members of an Independent and Assisted Living Community for Older Adults – Seattle, Washington, 2020. *MMWR Morb. Mortal. Wkly. Rep.* 69 (14), 416–418.
- Russell, T.W., Hellewell, J., Jarvis, C.I., Van Zandvoort, K., Abbott, S., Ratnayake, R., Flasche, S., Eggo, R.M., Edmunds, W.J., Kucharski, A.J., 2020. Estimating the infection and case fatality ratio for coronavirus disease (COVID-19) using age-adjusted data from the outbreak on the Diamond Princess cruise ship, February 2020. *Eurosurveillance* 25 (12), 2000256.
- Schreiber, S.J., Ke, R., Loverdo, C., Park, M., Ahsan, P., Lloyd-Smith, J.O., 2021. Cross-scale dynamics and the evolutionary emergence of infectious diseases. *Virus Evol.* 7 (1), veaa105.
- Supasa, P., Zhou, D., Dejnirattisai, W., Liu, C., Mentzer, A.J., Ginn, H.M., Zhao, Y., Duyvesteyn, H.M.E., Nutalai, R., Tuekprakhon, A., 2021. Reduced neutralization of SARS-CoV-2 B.1.1.7 variant by convalescent and vaccine sera. *Cell* 184 (8), 2201–2211. e2207.
- Tang, J.W., Tambyah, P.A., Hui, D.S., 2020. Emergence of a new SARS-CoV-2 variant in the UK. *J. Infect.* 82 (4), e27–e28.
- Tang, J.W., Toovey, O.T.R., Harvey, K.N., Hui, D.D.S., 2021. Introduction of the South African SARS-CoV-2 variant 501Y.V2 into the UK. *J. Infect.* 82 (4), E8–E10.
- Teslya, A., Pham, T.M., Godijk, N.G., Kretzschmar, M.E., Bootsma, M.C.J., Rozhnova, G., 2020. Impact of self-imposed prevention measures and short-term government-imposed social distancing on mitigating and delaying a COVID-19 epidemic: A modelling study. *PLoS Med.* 17 (7), e1003166.
- Tsetsarkin, K.A., Vanlandingham, D.L., McGee, C.E., Higgs, S., 2007. A single mutation in chikungunya virus affects vector specificity and epidemic potential. *PLoS Pathog.* 3 (12), e201.
- van den Driessche, P., Watmough, J., 2002. Reproduction numbers and sub-threshold endemic equilibria for compartmental models of disease transmission. *Math. Biosci.* 180, 29–48.
- Verity, R., Okell, L.C., Dorigatti, I., Winskill, P., Whittaker, C., Imai, N., Cuomo-Dannenburg, G., Thompson, H., Walker, P.G.T., Fu, H., et al., 2020. Estimates of the severity of coronavirus disease 2019: a model-based analysis. *Lancet Infect. Dis.* 20 (6), 669–677.
- Volz, E., Mishra, S., Chand, M., Barrett, J.C., Johnson, R., Geidelberg, L., Hinsley, W.R., Laydon, D.J., Dabbera, G., O'Toole, ., 2021a. Assessing transmissibility of SARS-CoV-2 lineage B.1.1.7 in England. *Nature* 593 (7858), 266–269.
- Volz, E., Hill, V., McCrone, J.T., Price, A., Jorgensen, D., O'Toole, A., Southgate, J., Johnson, R., Jackson, B., Nascimento, F.F., et al., 2021b. Evaluating the Effects of SARS-CoV-2 Spike Mutation D614G on Transmissibility and Pathogenicity. *Cell* 184 (1), 64–75 e11.
- Walensky, R.P., Walke, H.T., Fauci, A.S., 2021. SARS-CoV-2 Variants of Concern in the United States—Challenges and Opportunities. *JAMA* 325 (11), 1037.
- Wang, K., Zhao, S., Liao, Y., Zhao, T., Wang, X., Zhang, X., Jiao, H., Li, H., Yin, Y.i., Wang, M.H., et al., 2020. Estimating the serial interval of the novel coronavirus disease (COVID-19) based on the public surveillance data in Shenzhen, China, from 19 January to 22 February 2020. *Transbound. Emerg. Dis.* 67 (6), 2818–2822.
- Whittles, L.K., White, P.J., Didelot, X., 2017. Estimating the fitness cost and benefit of cefixime resistance in *Neisseria gonorrhoeae* to inform prescription policy: a modelling study. *PLoS Med.* 14 (10), e1002416.
- Wise, J., 2021. Covid-19: The E484K mutation and the risks it poses. *British Medical Journal Publishing Group*.
- Wu, J.T., Leung, K., Leung, G.M., 2020. Nowcasting and forecasting the potential domestic and international spread of the 2019-nCoV outbreak originating in Wuhan, China: a modelling study. *Lancet* 395 (10225), 689–697.
- Xie, X., Liu, Y., Liu, J., Zhang, X., Zou, J., Fontes-Garfias, C.R., Xia, H., Swanson, K.A., Cutler, M., Cooper, D., et al., 2021. Neutralization of SARS-CoV-2 spike 69/70 deletion, E484K and N501Y variants by BNT162b2 vaccine-elicited sera. *Nat. Med.* 27 (4), 620–621.
- Yadav, P.D., Sapkal, G.N., Abraham, P., Ella, R., Deshpande, G., Patil, D.Y., Nyayanit, D. A., Gupta, N., Sahay, R.R., Shete, A.M., et al., 2021. Neutralization of variant under investigation B.1.617 with sera of BBV152 vaccinees. *Clin. Infect. Dis.*
- Zhao, S., 2020. Estimating the time interval between transmission generations when negative values occur in the serial interval data: using COVID-19 as an example. *Math Biosci. Eng.* 17 (4), 3512–3519.
- Zhao, S., Stone, L., Gao, D., Musa, S.S., Chong, M.K.C., He, D., Wang, M.H., 2020. Imitation dynamics in the mitigation of the novel coronavirus disease (COVID-19) outbreak in Wuhan, China from 2019 to 2020. *Ann. Trans. Med.* 8 (7), 448.
- Zhao, S., Musa, S.S., Chong, M.K., Ran, J., Javanbakht, M., Han, L., Wang, K., Hussaini, N., Habib, A.G., Wang, M.H., et al., 2021. The co-circulating transmission dynamics of SARS-CoV-2 Alpha and Eta variants in Nigeria: A retrospective modeling study of COVID-19. *J. Glob Health.* 11, 05028.
- Zhao, S., Lou, J., Cao, L., Zheng, H., Chong, M.K.C., Chen, Z., Chan, R.W.Y., Zee, B.C.Y., Chan, P.K.S., Wang, M.H., 2021a. Quantifying the transmission advantage associated with N501Y substitution of SARS-CoV-2 in the UK: an early data-driven analysis. *J. Travel Med.* 28 (2), taab011.
- Zhao, S., Lou, J., Cao, L., Zheng, H., Chong, M.K.C., Chen, Z., Chan, R.W.Y., Zee, B.C.Y., Chan, P.K.S., Wang, M.H., 2021b. Modelling the association between COVID-19 transmissibility and D614G substitution in SARS-CoV-2 spike protein: Using the surveillance data in California as an example. *Theor. Biol. Med. Modell.* 8 (1), 10.